Tetracoordinated Bis-phenanthroline Copper-Complex Couple as Efficient Redox Mediators for Dye Solar Cells

Tetracoordinated bis-phenanthroline Copper-complex couple as efficient redox mediators for dye solar cells

Mirko Magni,[†,] Roberto Giannuzzi,[‡] Alessia Colombo,[†*] Maria Pia Cipolla,[‡] Claudia Dragonetti,[†] Stefano Caramori,[¥] Stefano Carli,[¥] Roberto Grisorio,[‡] Gian Paolo Suranna,[‡] Carlo Alberto Bignozzi,[¥] Dominique Roberto,[†] and Michele Manca[‡,*]*

[†] Dip. di Chimica, Università di Milano, UdR dell'INSTM, Via Golgi, Milano, Italy.

[‡] CBN-Fondazione Istituto Italiano di Tecnologia, Via Barsanti, Arnesano (Lecce), Italy.

[¥] Dip. Scienze Chimiche e Farmaceutiche, Università di Ferrara, Via F. di Mortara, Ferrara, Italy.

‡ Dip. di Ingegneria Civile, Ambientale, del Territorio, Edile e di Chimica, Politecnico di Bari, via Orabona, Bari and CNR-NANOTEC c/o Campus Ecotekne, via Monteroni, Lecce, Italy.

*Corresponding authors e-mail: **mirko.magni@unimi.it**; **alessia.colombo@unimi.it**; **michele.manca@iit.it**

ABSTRACT. A tetracoordinated redox couple, made by [Cu(2-mesityl-4,7-dimethyl-1,10-phenanthroline)$_2$][PF_6], **1**, and its Cu(II) form [Cu(2-mesityl-4,7-dimethyl-1,10-phenanthroline)$_2$][PF_6]$_2$, **2**, has been synthesized and its electrochemical and photochemical features have been investigated and placed in comparison with those of a previously published Cu^{2+}/Cu^{+} redox shuttle, namely [Cu(2,9-dimethyl-1,10-phenanthroline)$_2$][PF_6], **3**, and its pentacoordinated oxidized form [Cu(2,9-dimethyl-1,10-phenanthroline)$_2$Cl][PF_6], **4**. The

detrimental effect of the fifth Cl^- ancillary ligand on the charge transfer kinetics of the redox shuttles has been exhaustively demonstrated. Appropriately balanced Cu-based electrolytes have been then formulated and tested in DSCs in combination with a π-extended benzothiadiazole dye. The bis-phenanthroline Cu-complexes, **1** and **2**, have been found to provide an overall 4.4% solar energy conversion efficiency, which results more than twice that of the literature benchmark couple, **3** and **4,** employing a Cl-coordinated oxidized species and even comparable with the performances of a I^-/I_3^- electrolyte of analogous concentration. A fast counter-electrode reaction, due to the excellent electrochemical reversibility of **2**, and a high electron collection efficiency, allowed through the efficient dye regeneration kinetics exerted by **1**, represent two major prerogatives of these copper-based electron mediators and may constitute a pivotal step towards the development of a next generation of copper-based efficient iodine-free redox shuttles.

KEYWORDS: copper complexes, electron mediators, dye-sensitized solar cells, charge transfer kinetics, iodine-free electrolytes

Introduction

Electrolytes in liquid dye solar cells (DSCs) function as the medium to transfer electrons from the counter electrode to the oxidized dye chemisorbed on the photoanode, allowing cyclability of the device operation. Solubility and ionic mobility of the electron shuttle in the organic medium, driving force for the dye regeneration, and fast electron transfer kinetics with a minimal overpotential at the counter electrode are crucial factors in

determining the performances of the photoelectrochemical system. Since the milestone paper of O'Regan and Graetzel,[1] the sensitizer structure and the photoanode material have been the subject of considerable efforts aimed at increasing power conversion efficiencies.[2-6] On the contrary, for more than ten years the role of redox mediators is passed largely into the background, since the iodide–triiodide ($\mathbf{I^-/I_3^-}$) couple had been recognized as the most universal redox shuttle because of its satisfactory kinetic properties (such as fast oxidation of I^- and slow reduction of I_3^- at the photoanode/electrolyte interface), excellent infiltration, relative high stability, low cost and easy preparation. Despite this, several shortcomings exist for the I^-/I_3^- electrolyte. Disadvantages such as the absorption of visible light (due to the tail of the UV band of I_3^- in the 350-450 nm region), corrosiveness, and mediator/dye mismatched half-wave potentials resulting in an upper limit on open circuit potential, V_{oc}, of *ca.* 0.9 V, significantly restrict further development of DSCs using this electrolyte system.[7-9]

As a result, the search for alternative efficient electron shuttles is of crucial importance and it is attracting more and more attention, being identified as the potential turning point toward fabrication of high performing DSCs.[10] In this frame, several alternative electrolytes have been investigated,[8] including first-row transition metal complexes[11] due to both the high ductility of their electrochemical features by changing ligands and/or central atom, and the relatively low cost of the earth-abundant metals such as Ni,[12] Fe,[13] Co[9,14-17] and Cu.[18-21]

In 2011, the tris(bipyridyl)Co(II/III) redox couple contributed to a remarkable photon-to-current conversion efficiency, PCE, of 12.3% for liquid DSCs with a V_{oc} greater than 0.9 V,[16] neatly improving the stagnant 11% topmost efficiency recorded by I^-/I_3^- electrolyte-based DSCs.[22] Since then, several related studies of Co(II/III) complex electrolytes have

been performed, extending research to a great variety of engineered chelates including also tridentate, pentadentate, and exadentate pyridyl ligands.[23-25] Finally, very recently, the threshold value of 14% has been exceeded.[14] To date cobalt tris(diimine) redox couples undisputed hold leadership of iodide-free electrolytes for liquid DSCs,[26] even if their relatively low diffusion coefficients, fast photo-excited electron recapture at photoanode interface along with long-term stability concerns make cobalt complex couples a still open field of reseach.[27]

In this challanging study of novel electron shuttles, copper complexes could be intriguing alternatives. Copper is intrinsically less toxic than cobalt, and its complexes are generally characterized by different preferred geometries depending on the oxidation state of the metal (*i.e.* typically Cu(I), with a d^{10} configuration, or Cu(II), d^{9}) resulting in electron transfer (ET) processes with high internal reorganization energies. This last feature, if properly tuned, makes copper complexes particularly appealing because they can meet the contrasting kinetic criteria, the so-called kinetic dichotomy, requiring both fast dye (and mediator) regeneration and slow charge recombination at the photoanode interface, by judicious tuning of their electron transfer rate and redox potential through ligand tailoring.[7,28]

To the best of our knowledge, notwithstanding the paramount role covered by copper in biological ET processes with “blue copper proteins”,[29] only a few recent papers have reported the implementation of properly designed copper complexes as electron mediators[18-20] and solid hole conductor[21] in DSCs. Yet, sterically hindered ligands endow these coordination compounds with suitable oxidation potentials[30] and self-exchange ET rates[18] compatible with their use as redox shuttles in DSCs.

The very modest PCEs obtained in the pioneering work of Hattori *et al.* with blue copper model complexes,[18] were neatly improved in 2011 by Wang and co-workers who formulated a Cu(I)/Cu(II)-based electrolyte for DSCs, employing [Cu(2,9-dimethyl-1,10-phenanthroline)$_2$]$^+$ complex and its chlorine-coordinated oxidized form [Cu(2,9-dimethyl-1,10-phenanthroline)$_2$Cl]$^+$, able to reach remarkable power conversion efficiency.[19] It is to be noted that in the latter complex an ancillary ligand (*i.e.* Cl^-) was mandatorily introduced to stabilize the Cu(II) complex allowing its isolation and storage (otherwise impossible due to a fast, interconversion into its cuprous counterpart) but, surprisingly, the electrochemical implication of such ligand had never been reported yet.

Since then the already scarce literature has exclusively focused on the aforementioned prototype couple based on the 2,9-dimethyl-1,10-phenanthroline ligand, omitting any other possible derivates of the condensed core. Hence, a long-term study has been devoted to rationalize how modifications of bis-phenanthroline copper complexes and/or additive addition can influence DSC efficiencies filled with copper-based electrolytes.

In our previous report we demonstrated that [Cu(2-mesityl-4,7-dimethyl-1,10-phenanthroline)$_2$][PF_6], **1**, (Chart 1) together with its Cu(II) form, which was obtained through the addition of $NOBF_4$ to the electrolyte solution, can act as suitable redox mediators, their performance depending on the nature of the dye.[20]

In this work, having the aim of achieving a fine control of the electrolytes composition as well as of more deeply investigating the relationship between the charge transfer features of each of their components and the overall cell efficiency, we focused on the synthesis of the tetracoordinated Cu(II) complex [Cu(2-mesityl-4,7-dimethyl-1,10-phenanthroline)]$^{2+}$ (see compound **2** in Chart 1) which had never been isolated so far.

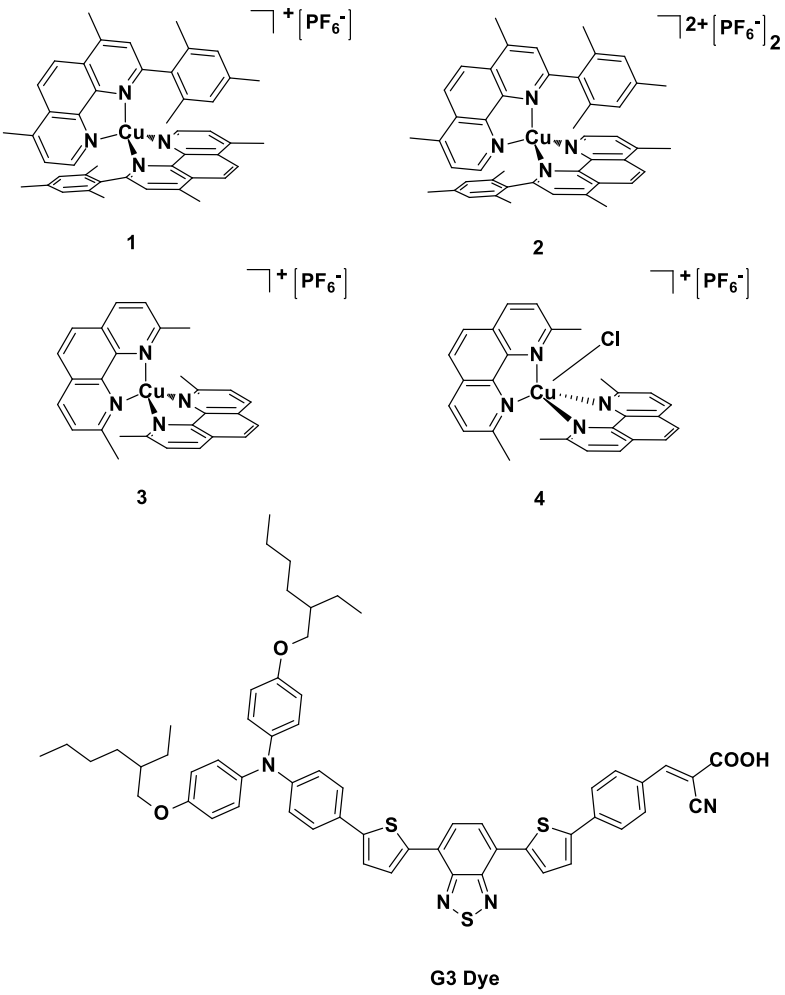

Chart 1. Structures of the copper complexes (**1**-**4**) and of the dye (**G3**, bottom) investigated.

A comparative electrochemical study of two couples of copper complexes, **1**/**2** and **3**/**4**, has been carried out. As a result the kinetics prerogatives associated to the tetracoordinated cupric complex (*i.e.* **2**) instead of the pentacoordinated species (*i.e.* **4**) will be exhaustively discussed. Finally implication of such differences have been studied in DSCs, through the comparison of photoelectrochemical performances of liquid DSCs filled with an optimized **1**/**2**-based electrolyte and with a benchmark **3**/**4**-mixture, in combination with a benzothiadiazole based donor-π-acceptor organic dye, namely **G3**

(see Chart 1), which has been recently shown to exhibit very promising solar energy conversion efficiencies.[31]

Experimental Methods

Synthesis of copper complexes

All reagents were purchased from Sigma-Aldrich and were used without further purification. Reactions requiring anhydrous conditions were performed under argon. The preparation of complexes **1**, **3** and **4** is reported in the Supporting Information (SI) and in previous publications,[19,20] whereas the synthetic procedure of **2** is reported below.

Synthesis of Cu(II) complex 2. The 2-mesityl-4,7-dimethyl-1,10-phenanthroline ligand[20] (0.15 mmol) was dissolved in dry CH_3CN (5 mL) and a solution of $CuSO_4*5H_2O$ (0.075 mmol) in 1.5 mL of water was slowly added. The green solution was stirred at room temperature for 2 h and then concentrated at reduced pressure to 1.5 mL and $NaPF_6$ (0.40 mmol) was added forming immediately a green precipitate. After 1 hour the mixture was filtered and the solid was washed three times with water and then with diethyl ether. The product was obtained in 60% yield.

Elemental analysis: Calcd. for $C_{46}H_{44}CuF_{12}N_4P_2$: C, 54.90; H, 4.41; N, 5.57; found: C, 55.01; H, 4.38; N, 5.44; ESI(+) FTICR MS(*m*/*z*) calcd. for $[C_{46}H_{44}CuN_4]^{2+}$ 715.2862 found 715.2859.

Elemental analysis and mass spectra were obtained with PERKINELMER 2004 Series II CHNS/O Analyzer and LTQ FT Ultra (7Tesla) Thermo Scientific mass spectrometer respectively.

Characterization and solar device details

Electrochemical characterization. Three-electrode measurements (cyclic voltammetry, CV, and electrochemical impedance spectroscopy, EIS) were performed in minicell filled with 2-4 cm^3 of working solution equipped with a working electrode, a Pt-foil counter electrode and an aqueous saturated calomel electrode, SCE, as operative reference electrode. SCE was inserted into a glass jacket (ending in a porous frit) filled with the same blank solution employed in cell, in order to avoid leakage of both water and chlorides into the working medium. Different working electrodes were employed: teflon-embedded glassy carbon disk electrode (GC, Metrohm, geometric area 0.071 cm^2); glass-embedded platinum disk electrode (Pt, Metrohm, 0.0341 cm^2); PEDOT-coated GC or Pt electrodes were prepared by potentiodynamic electrodeposition in a EDOT solution (See SI). The recorded potentials were all referred to the intersolvental reference redox couple ferricenium/ferrocene, Fc^+/Fc;[32] in our conditions the half-wave potential of the Fc^+/Fc couple was *ca.* 0.39 V and 0.31 V *vs* SCE in $TBAPF_6$ and $LiClO_4$ solution, respectively.

Experiments were performed using Autolab PGSTAT 302N potentiostats/galvanostats (EcoChemie, The Netherlands) managed by a PC with GPES or NOVA software. During CV measurements ohmic drop between working and reference electrodes was minimized by instrumental compensation via positive-feedback technique. The staircase CVs were performed with a 0.001 V step potential. EIS measurements were recorded using 60 logarithm-spaced single wave frequencies from 100 kHz to 0.1 Hz, with 0.01 V amplitude. EIS data were analyzed with NOVA software.

All measurements were performed in acetonitrile (anhydrous, Sigma Aldrich, 99.8%) with 0.1 M tetrabutylammonium hexafluorophosphate ($TBAPF_6$, Sigma Aldrich, ≥98.8%)

or lithium perchlorate ($LiClO_4$, Sigma Aldrich, ≥98.0%) as supporting electrolytes; complex concentrations were around 0.001 M. Before starting measurements, solution was well-deareated by nitrogen bubbling.

Dye solar cells fabrication. Fluorine-doped tin oxide, FTO, coated glass (15 Ω sq^{-1}, purchased from XIN YAN TECHNOLOGY LTD) were cleaned in a detergent solution for 15 min and in ethanol for 30 min using an ultrasonic bath. Mesoporous TiO_2 electrodes were prepared by doctor blading a commercial paste (30NRD, Dyesol) and subjecting them to thermal sintering at 430 °C for 40 min. The average thickness of the electrodes used in the reported batch of devices was 12 μm (DEKTAK 150TM profilometer). After first thermal sintering all the samples were treated with a 40 mM aqueous solution of $TiCl_4$ for 30 min at 60° C, rinsed again with water and ethanol and then subjected to a second sintering process at 480°C for 30 min. After cooling to 80 °C the mesoporous electrodes were immersed into the dye solution (0.2 mM of **G3** added to 30 mM chenodeoxycholic acid in tetrahydrofuran) for 8 h. The counter electrodes were prepared by sputtering a 50 nm Pt layer on a hole-drilled cleaned FTO plate. Two electrodes were then assembled together in a sandwich configuration and sealed upon heating a thermoplastic gasket made of a hot-melt ionomer-class resin (Surlyn 50-μm thickness). The electrolytic solution was injected through the hole on the counter electrode glass.

Tests under illumination were made using a Newport Sol3A Class AAA Solar Simulator (Model 94063A equipped with a 1000W xenon arc lamp). More details are reported in SI.

Electrolyte preparation. Copper-containing electrolytes, **1**/**2** EL and **3**/**4** EL, were prepared by dissolving the desired Cu(I) complex (0.17 M) in a suitable amount of ACN

with $LiClO_4$ 0.1 M. After that the calculated amount of Cu(II) counterpart (0.017 M) was added and stirred until dissolution. A Rd/Ox 10:1 molar ratio was so obtained. Suitable volumes of 4-*tert*-butylpyridine, *t*-bpy, were finally added to reach 0.25 M concentration in the electrolyte solutions. Iodine-based electrolyte $\mathbf{I^-/I_3^-_{equim}}$ (with a I^-/I_2 molar ratio=10:1) was prepared in a similar way mixing 0.017 M of I_2 with 0.17 M of 1,2-dimethyl-3-propylimidazolium iodide, DMPII, 0.1 M of $LiClO_4$ and 0.25 M of *t*-bpy in ACN. The highly concentrated $\mathbf{I^-/I_3^-_{conc}}$ EL was instead composed of I_2 0.07 M, DMPII 0.7 M, LiI 0.2 M and *t*-bpy 0.5 M.

Transient absorption spectroscopy measurements. Transient absorption spectroscopy, TAS, was performed with a previously described apparatus.[33] Excitation of the sensitized TiO_2 films was carried out by using the 532 nm radiation generated by a Continuum Surelite (II) Nd-YAG laser, pumped at 1.26 kV. Set up is well described in SI. Sensitized substrates for TAS were obtained by dipping freshly annealed (180 °C, 30 min.) 4 μm thick TiO_2 films in a THF solution containing 0.2 mM **G3** dye and 30 mM chenodeoxycholic acid. The adsorption was carried out overnight in the dark at room temperature. Four different solutions were prepared for observing the regeneration kinetics of **G3** loaded on TiO_2 electrodes: i) a blank ACN + $LiClO_4$ 0.1 M solution; ii) a 0.17 M solution of complex **1** in ACN with $LiClO_4$ 0.1 M; iii) a 0.17 M solution of complex **3** in ACN with $LiClO_4$ 0.1 M; iv) a 0.7 M solution of $\mathbf{I^-}$ obtained mixing 0.6 M of DMPII, and 0.1 M of LiI in ACN. These electrolytes were drawn by capillary forces into the micrometric spacing between the TiO_2 photoanode and a microscope slide pressed over it, which also protected the TiO_2 surface from direct air exposure.

TAS of the **G3** excited state in 0.2 mM in aerated THF solution were obtained with the same spectrometer and experimental setup, except that both the excitation and the probe beams were not attenuated.

Results and Discussion

Spectroscopic and electrochemical characterization

The synthesis and the characterization of complexes **1**-**4** are detailed in the Supporting Information (SI). The UV-Vis absorption spectra (Fig. 1a) in acetonitrile, ACN, show *d*-*d* transitions of Cu(II) species red-shifted (λ_{max}=697 and 741 nm, for **2** and **4**, respectively) and weaker ($\varepsilon_{max}\approx$100 and 200 M^{-1} cm^{-1}, for **2** and **4**) than the MLCT transitions[34] found in the parent Cu(I) complexes, falling at 445 nm with $\varepsilon_{max}\approx 4.5\cdot10^3$ M^{-1} cm^{-1} for **1** and at 455 nm with $\varepsilon_{max}\approx 8\cdot10^3$ M^{-1} cm^{-1} for **3**. The less intense absorption of the 2-aryl substituted complex **1** respect to **3** is in good agreement with literature findings.[35,36] From the electrochemical point of view bis-phenanthroline Cu-complexes in a 0.1 M $TBAPF_6$ solution in ACN (Fig. 1b) are characterized by ligand-based ETs occurring in the cathodic window and by a metal-centred process located in the anodic region.[30] Complex **1** and its oxidized form **2** exhibit an identical oxidation half-wave potential, $E_{1/2}$, of −0.02 V *vs* $Fc^+|Fc$, confirming their mutual interconversion during the ET process. Conversely, besides a good superimposition of the two ligand-based processes, a clear different behavior is detected for the metal-centred process, with a remarkable lower electrochemical reversibility for compound **4** respect to **3**, coupled with a more negatively shifted half-wave potential ($E_{1/2}$=0.30 V and 0.04 V *vs* $Fc^+|Fc$ for **3** and **4** respectively).

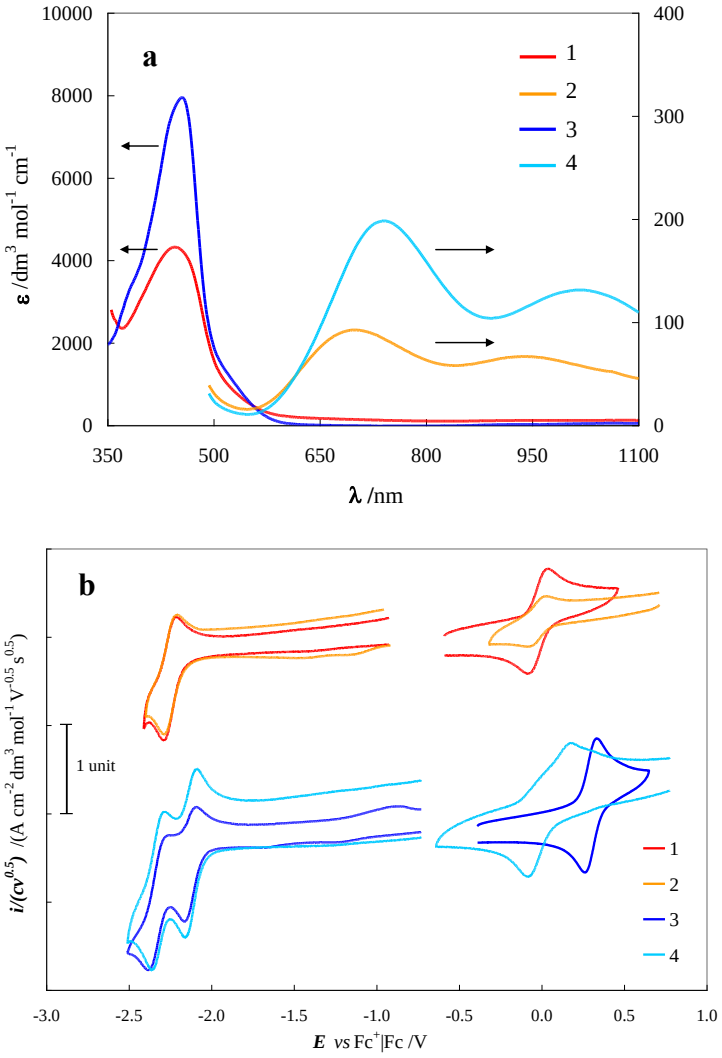

Fig. 1 a) Normalized electronic absorption spectra of cuprous (**1** and **3**) and cupric (**2** and **4**) complexes in ACN. b) Normalized cyclic voltammograms, CVs, of **1**-**4** (0.001 M) on glassy carbon, GC, electrode in ACN with $TBAPF_6$ 0.1 M. Scan rate potential 0.2 V s^{-1}.

This behavior is indeed associated to the presence of the chloride ligand into the coordination sphere of copper. In fact the resulting tetragonal pentacoordinated geometry stabilizes the Cu(II) form making the reduction of **4** thermodynamically less favourable than in homologous **3** but, at the same time, it slows down the ET kinetics of **4** presumably due to the higher reorganization energy deriving from the dissociation of the

Cl^- during Cu^{2+}/Cu^+ switch (Fig. S1, SI). As a matter of fact, progressive addition of sub-stoichiometric chloride ions to a solution of **3** turns into a progressive intensification of the negatively shifted redox waves, and to a linear decrease of the pristine fingerprints of **3**, which even disappears at Cl^- concentrations higher than 1.0 equivalent, thus attesting the full conversion of **3** in **4** (Fig. 2 and Fig. S2)

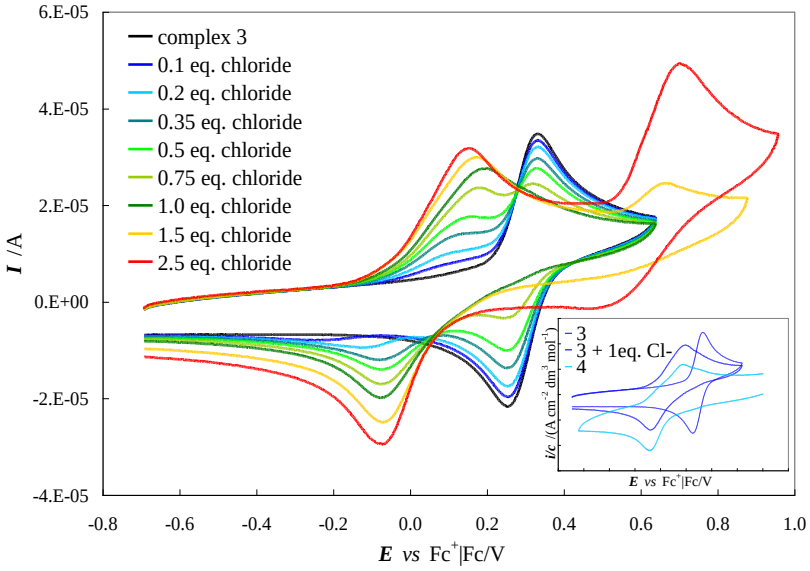

Fig. 2 CVs of complex **3** at increasing amount of chloride ions spiked in the working medium as TBACl solution. Inset: synopsis of normalized CVs showing the equivalence of complex **4** (light blue thick line) with the species obtained adding 1.0 eq. of Cl^- to a solution of complex **3** (blue thick line); for sake of comparison the CV of the same pristine complex **3** is reported (blue thin line). In all cases: 0.2 V s^{-1} scan rate potential.

Effect of 4-*tert*-butylpyridine. In view of a reliable implementation of the coordinatively unsaturated complex **2** as redox mediators in DSCs, the coordination ability of 4-*tert*-butylpyridine, *t*-bpy, (commonly added to electrolytes to increase the open circuit potential of cell)[37] has been investigated. The proof of a N-heterocyclic Lewis base coordination to a metal

center has been reported for a cobalt-based complex redox couple,[24] causing a negative shift of $E_{1/2}$, as well as an increase in the electrochemical irreversibility of the ET. Differently from what observed with the addition of Cl^- (Fig. S3), amount of *t*-bpy up to an equimolar threshold into solutions of both **1** and **2** does not bring to significant variation in their $E_{1/2}$ (Fig. 3 and Fig. S4).

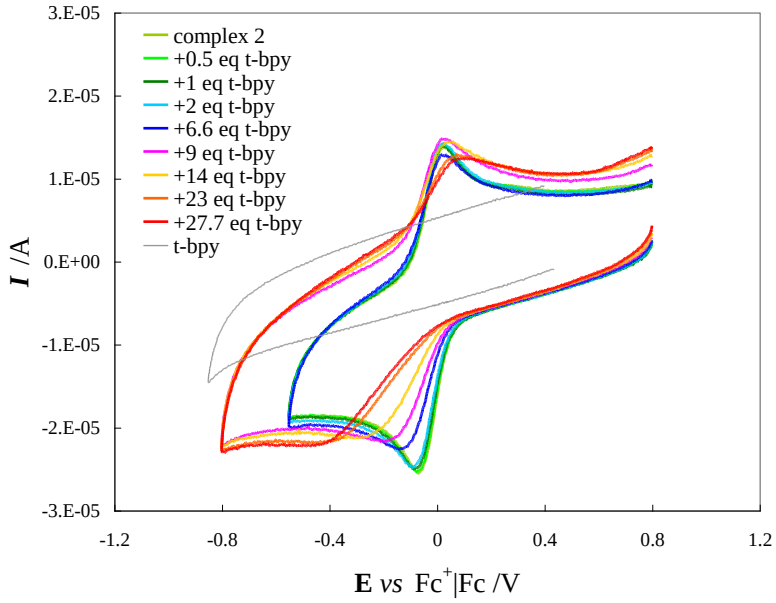

Fig. 3 Normalized CVs for complex **2** in ACN with $LiClO_4$ 0.1 M after subsequent additions of *t*-bpy. GC electrode; potential scan rate 0.2 V s^{-1}.

This difference can be attributed to the stronger coordination ability of chloride ions[38] respect to the bulkier and neutral Lewis base. On the contrary, at concentration of *t*-bpy comparable to that employed in DSCs' electrolytes (*i.e.* around 15-times higher than Cu(II) complex concentration) a negative shift and a broadening of the cathodic peak appear (Fig. 3). These observations can prove a labile coordination of the base to Cu(II) centre that, similarly to aforementioned chloride case, slows down the ET as a consequence of the significant geometry modification induced by formation/dissociation

of the adduct. This finding suggests that the addition of *t*-bpy may be beneficial for the use of these complexes as electrolytes in DSCs, since it induces a reduction of parasitic interfacial charge recombination processes, not only through adsorbing on the TiO_2 surface, but also by direct interaction with the oxidized form of the mediator.

Counter electrode electron transfer kinetics. ET kinetic of the metal-centred processes was then investigated by electrochemical impedance spectroscopy, EIS, (Fig. S6) on glassy carbon electrode, GC, taken as an ideally inert electrode material, with a classical three-electrode configuration (See SI). A remarkably faster ET was detected in the case of **3** with respect to **1**, with charge transfer resistance, R_{ct}, at half-wave potential of *ca.* 14 Ω cm^2 and 40 Ω cm^2 respectively, calculated fitting impedance spectra with a Randles equivalent circuit.[39] This difference can be reasonably attributed to the higher steric hindrance offered by the four methyl groups in **3** in comparison to the two mesityl rings of **1**, which may induce a smaller conformational modification upon the redox reaction, acting as a "kiss-lock enclosure" that causes an increase of the $E_{1/2}$ (Fig. 1b) due to a destabilization of the electrogenerated Cu(II) species[30] but, at the same time, a reduction of the activation barrier for the ET.

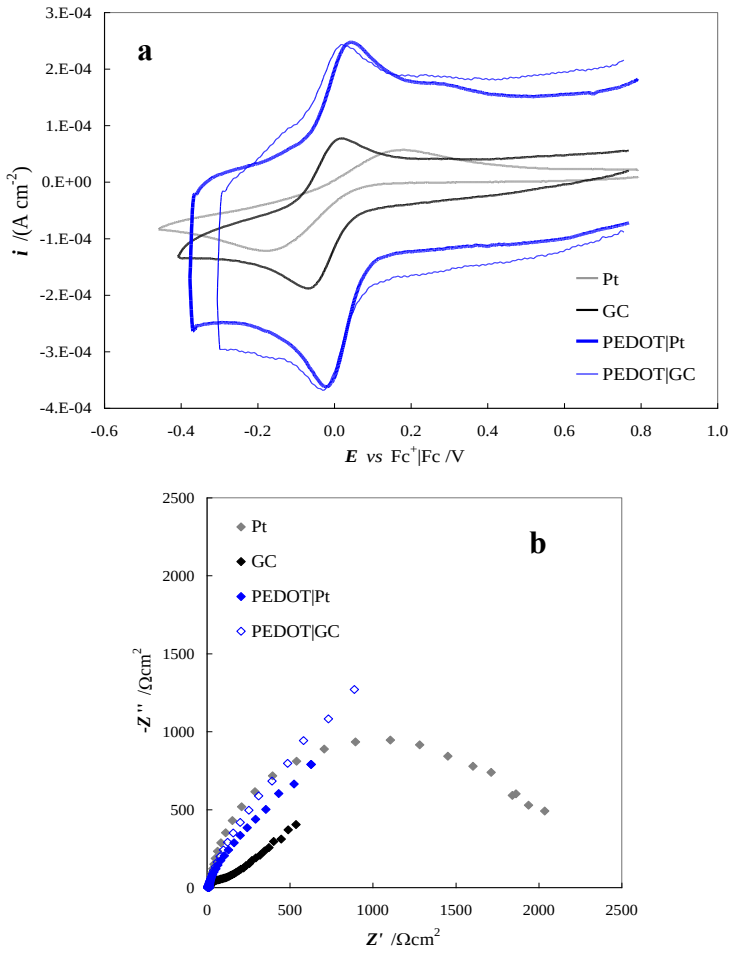

Fig. 4. a) Normalized CVs (at 0.05 V s^{-1}) and b) Nyquist diagrams at $E_{1/2}$ of **2** in ACN with $LiClO_4$ 0.1 M recorded on different electrode supports: Pt (grey line), GC (black line), PEDOT electrodeposited on Pt (blue thick line) and PEDOT electrodeposited on GC (blue thin line).

One of the primary requirements of the electron shuttles is a fast regeneration of the redox mediator at the counter electrode, CE, where the ET should occur with minimal overpotential losses to improve the fill factor, *FF*, of the photoelectrochemical device. Platinum and poly(3,4-ethylendioxy)thiophene, PEDOT, coated FTO are among preferred cathodic material for DSCs.[40,41] Voltammetric plots recorded in ACN with $LiClO_4$ as supporting electrolyte (the same medium employed in DSC tests) showed in Fig. 4a

demonstrate that Pt is not the best catalyst for the reduction of compound **2** if compared to PEDOT and GC (taken as reference), since it exhibits a slightly higher activation barrier to the ET process, as confirmed by the larger separation of the voltammetric peaks and, consequently, by the higher value of R_{ct} (*ca.* $1 \cdot 10^2$ Ω cm^2 and *ca.* $2 \cdot 10^3$ Ω cm^2 for GC and Pt respectively) evaluated by EIS (Fig. 4b and Fig. S7). On the contrary, species **2** presents on PEDOT-coated working electrode (obtained through potentiodynamic electrodeposition, see SI) an almost reversible ET fingerprint (Fig. S8), which is independent from the material used as underlying substrate (namely GC or Pt).

Tests carried out on symmetrical sandwich-type cells fabricated with either PEDOT or Pt coated FTOs filled with **1**/**2** and **3**/**4** based ELs employed for application in DSCs, corroborate these findings and confirm that PEDOT-modified cathodes allow one order of magnitude faster regeneration of Cu-based redox mediators with respect to Pt-modified ones (Table 1 and Fig. S9). However electrodeposited PEDOT films present a slightly higher sheet resistance, R_{series}, with respect to sputtered Pt coatings. These two opposite features balance each others resulting in almost comparable overall impedance values. **3**/**4**-based EL show invariably higher R_{ct} values than **1**/**2** due to the aforementioned slow kinetics induced by the coordinated Cl^- in complex **4**; moreover, interestingly, the R_{ct} of **1**/**2** in combination with PEDOT electrodes invariably results one order of magnitude lower than that measured for an equimolar iodide-based electrolyte (Table 1).

Table 1. Fitted parameters[a] from EIS spectra for Pt-Pt and PEDOT-PEDOT symmetrical cells (active area 1 cm^2) at open circuit potential.

Electrolyte[b]	**Cathode**	R_{series} /Ω	R_{CE} /Ω	C_{CE} x 10^5 /F	R_d /Ω
1/**2**	Pt	21	9.8	4.05	12.8
1/**2**	PEDOT	37	0.82	232	14.2
3/**4**	Pt	39	61	1.28	164
3/**4**	PEDOT	53	4.4	500	223
$\mathbf{I^-/I_3^-}_{equim}$	Pt	30	11	2.2	11.2
$\mathbf{I^-/I_3^-}_{equim}$	PEDOT	55	8.2	$1.9\cdot10^2$	11.5
$\mathbf{I^-/I_3^-}_{conc}$[c]	Pt	26	0.82	3.6	2.05
$\mathbf{I^-/I_3^-}_{conc}$[c]	PEDOT	53	0.61	$5.0\cdot10^3$	2.38

[a]Using the classical Randles equivalent circuit. R_{CE} and C_{CE} values from fitting have been divided and multiplied, respectively, for a factor of 2 accounting for the symmetry of the cell. [b]Red/Ox molar ratio = 10:1 with [Red] = 0.17 M in ACN, $LiClO_4$ 0.1 M, *t*-bpy 0.25 M; for I^-/I_3^--based electrolytes Red=DMPII+LiI and Ox= I_2. [c]DMPII 0.8 M, LiI 0.2 M, I_2 0.07 M; *t*-bpy 0.5 M in ACN.

Transient absorption spectroscopy study

The comparative evaluation of the dye regeneration kinetics by the electrolytes under investigation was carried out by transient absorption, TA, spectroscopy on **G3** sensitized transparent TiO_2 films in contact with the electron donating electrolytes in ACN (*i.e.* **1**, **3**, and $\mathbf{I^-}$). The signature of the charge transfer triplet excited state measured in solution is reported on Fig. S10.

The transient spectrum (Fig. 5a) of the photooxidized dye on the TiO_2 surface, in the absence of electron mediators (*i.e.* charge separated state), shows features reminiscent of the charge transfer triplet state. In particular, the strong absorption in the red portion of the visible spectrum indicates the formation of the oxidized tri-arylamine, following charge injection into TiO_2.[42,43] Transient spectra of **G3** in the presence of Cu(I) and Cu(II) redox electrolytes are given in Figures S11-S13. 730 nm decays (Fig. 5b) of the oxidized dye in inert electrolyte provides an amplitude weighted lifetime, $\tau_{2/3}$, of *ca.* 1180 ns.

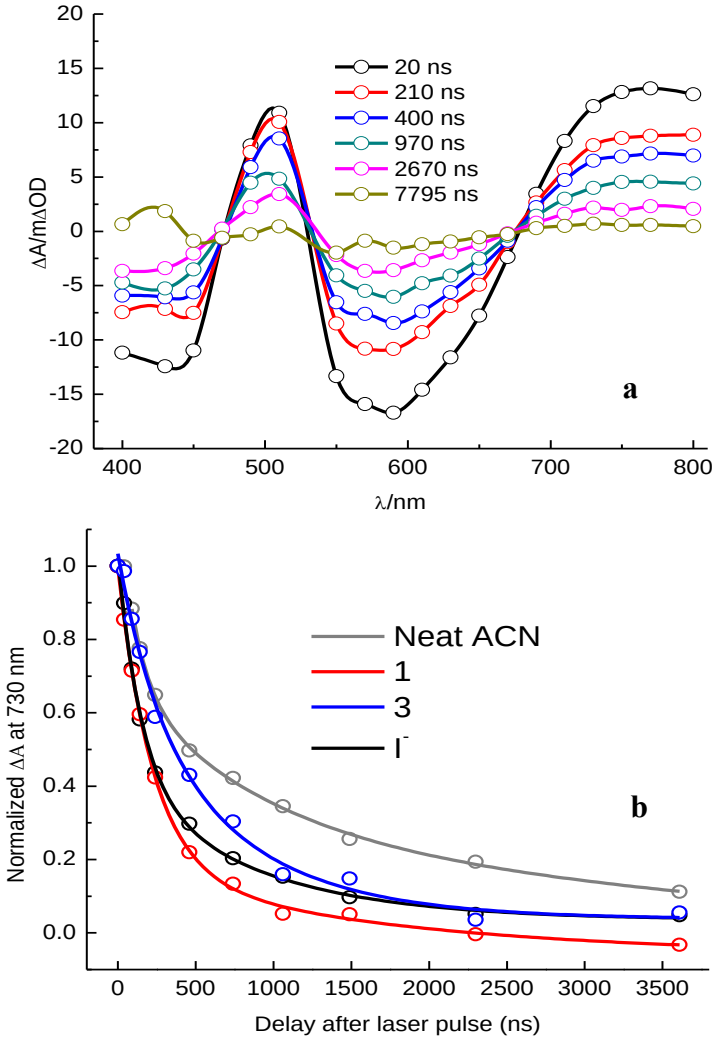

Fig. 5. a): Transient difference absorption spectra of **G3** dye loaded on transparent TiO_2 film in contact with inert ACN/0.1 M $LiClO_4$ electrolyte (blank). b): **G3** regeneration kinetics at 730 nm in the presence of ACN (blank, grey line), and in the presence of 0.17 M **1** (red), 0.17 M **3** (blue) and 0.7 M iodide (black). In all cases $LiClO_4$ 0.1 M was added. λ_{exc}=532 nm. Energies 1.5±0.5 mJ cm^{-2} $pulse^{-1}$.

The presence of reducing species (*i.e.* **1**, **3** and $\mathbf{I^-}$) induces, as expected, an acceleration of the oxidized dye's absorption decay due to electron donation from the redox mediators. Complex **1** (in 0.17 M concentration) afforded a **G3** regeneration efficiency, η_{reg}, of *ca.* 70% comparable with that calculated for the 0.7 M iodide solution. Compared to **1**, complex **3** exhibits a much lower dye regeneration efficiency (η_{reg}=45%) which can be mainly attributed to its *ca.* 0.3 eV lower driving force.

Dye solar cells tests

The Cu redox shuttles **1**/**2** and **3**/**4** were tested in **G3**-sensitized solar cells under AM 1.5G illumination. The branched alkyl chains of the dye are expected to reduce the parasitic charge recombination reactions of **2** (and **4**) at the photoanode while, at the same time, its high dipolar nature promotes both the electron/hole separation (thereby reducing direct back-electron transfer) and the dye regeneration.[31]

Chemical and electrochemical stability of the novel **1**/**2**-based electrolyte was verified into a symmetrical Pt|EL|Pt cell by cycling the potential between –1 and +1 V for 500 times (Fig. S14).

The photoelectrochemical performances of copper-based electrolytes were compared with those of a $\mathbf{I^-/I_3^-}$-based EL, $\mathbf{I^-/I_3^-_{equim}}$, which contained the $\mathbf{I^-/I_3^-}$ couple in equimolar

concentration to the Cu(I)/Cu(II) ELs. The results obtained for a DSC employing a ×6 concentrated $\mathbf{I^-/I_3^-}$ electrolyte formulation, $\mathbf{I^-/I_3^-_{conc}}$, is also reported for comparison (Table 2).

Table 2. **G3**-based DSCs (area=0.16 cm^2). Irradiation=100 mW cm^{-2} simulated AM 1.5G.

Electrolyte	Counter Electrode	PCE %	*FF*	V_{oc} /V	i_{sc} /mA cm^{-2}
1/**2**	Pt	4.4	0.66	0.72	9.3
1/**2**	PEDOT	4.1	0.67	0.74	8.2
3/**4**	Pt	1.9	0.59	0.86	3.8
$\mathbf{I^-/I_3^-}_{equim}$	Pt	4.3	0.70	0.70	8.7
$\mathbf{I^-/I_3^-}_{conc}$	Pt	7.4	0.67	0.72	15.4

1/**2**-based EL in combination with a Pt CE exhibits a power conversion efficiency, PCE, of 4.4%, comparable with the reference cell filled with the $\mathbf{I^-/I_3^-_{equim}}$, reaching 4.3% (Fig. 6a). In cells equipped with a PEDOT-coated CE, the **1**/**2** couple generated a lower i_{sc} with respect to an equivalent cell based on a reflective Pt sputtered counter electrode, mainly due to reduced light back scattering of partially transparent PEDOT. The decreased i_{sc} observed in the PEDOT-based DSCs is however partly offset by a slightly improved V_{oc} (from 0.72 V to 0.74 V). The almost identical *FF* values detected for two different CEs are justified by the higher sheet resistance of the PEDOT layer that perfectly counterbalances its faster ET, as discussed above. By contrast, **3**/**4**-based EL presented a much lower photocurrent density (i_{sc}=3.8 mA cm^{-2}) but a higher photovoltage (V_{oc}=0.86 V) consistent with the more positive Fermi level of the CE. Its overall 1.9% PCE was however inadequate with respect to the other electrolytes.

A **G3**-sensitized Pt-based DSC employing $\mathbf{I^-/I_3^-_{conc}}$ afforded 7.4% PCE (Table 2). It can be mainly attributable to the larger i_{sc}=15.4 mA cm^{-2}, which doubles that of $\mathbf{I^-/I_3^-_{equim}}$, suggesting that the Cu(I)/(II) complexes may be limited by their relatively low solubility in ACN. Indeed a solubility threshold of *ca*. 0.17 M was found for [Cu(2-mesityl-4,7-dimethyl-1,10-phenanthroline)$_2$][PF_6].

EIS analysis of these devices allows separating the most relevant factors affecting their photoelectrochemical performances and enables the independent study of the photoelectrode/electrolyte interfacial properties.[44] From Nyquist plots of DSCs measured under AM 1.5G at V_{oc} (Fig. 6b), it can be outlined that the high diffusional resistance, R_{diff}, (semi-arch at low frequencies) exhibited by **3**/**4**-based EL plays a detrimental role in the overall cell performances, in particular by lowering the *FF*. By contrast, **1**/**2** EL exhibits a remarkably lower R_{diff}, which is comparable with that detected in the cell based on $\mathbf{I^-/I_3^-_{equim}}$. In agreement with the superior charge transfer kinetics, leading to more efficient charge separation, **1**/**2** resulted in a TiO_2 chemical capacitance, C_{meas}, about one order of magnitude higher with respect to that obtained in the presence of **3**/**4** (Fig. S15). Values of the R_{ct} as a function of the corrected applied bias across the photoanode, are given in Fig. S15 too.

The **3**/**4**-based EL shows the highest R_{ct}, which accounts for the better V_{oc}. Similarly, $\mathbf{I^-/I_3^-_{equim}}$ presents the lowest R_{ct} while $\mathbf{I^-/I_3^-_{conc}}$ and **1**/**2**-based EL show almost the same values. Calculation of the transfer factor, β, from the voltage dependence of TiO_2 recombination resistance through the Tafel's law[45] gives β=0.4 for **1**/**2**-based devices, β=0.23 for **3**/**4**, β=0.53 for $\mathbf{I^-/I_3^-_{conc}}$, β=0.47 for $\mathbf{I^-/I_3^-_{equim}}$. The remarkably low value of β

factor in **3**/**4**-based EL constitutes a further quantitative assessment of the slow ET kinetics of the Cl^{-}-coordinated oxidized complex **4**.

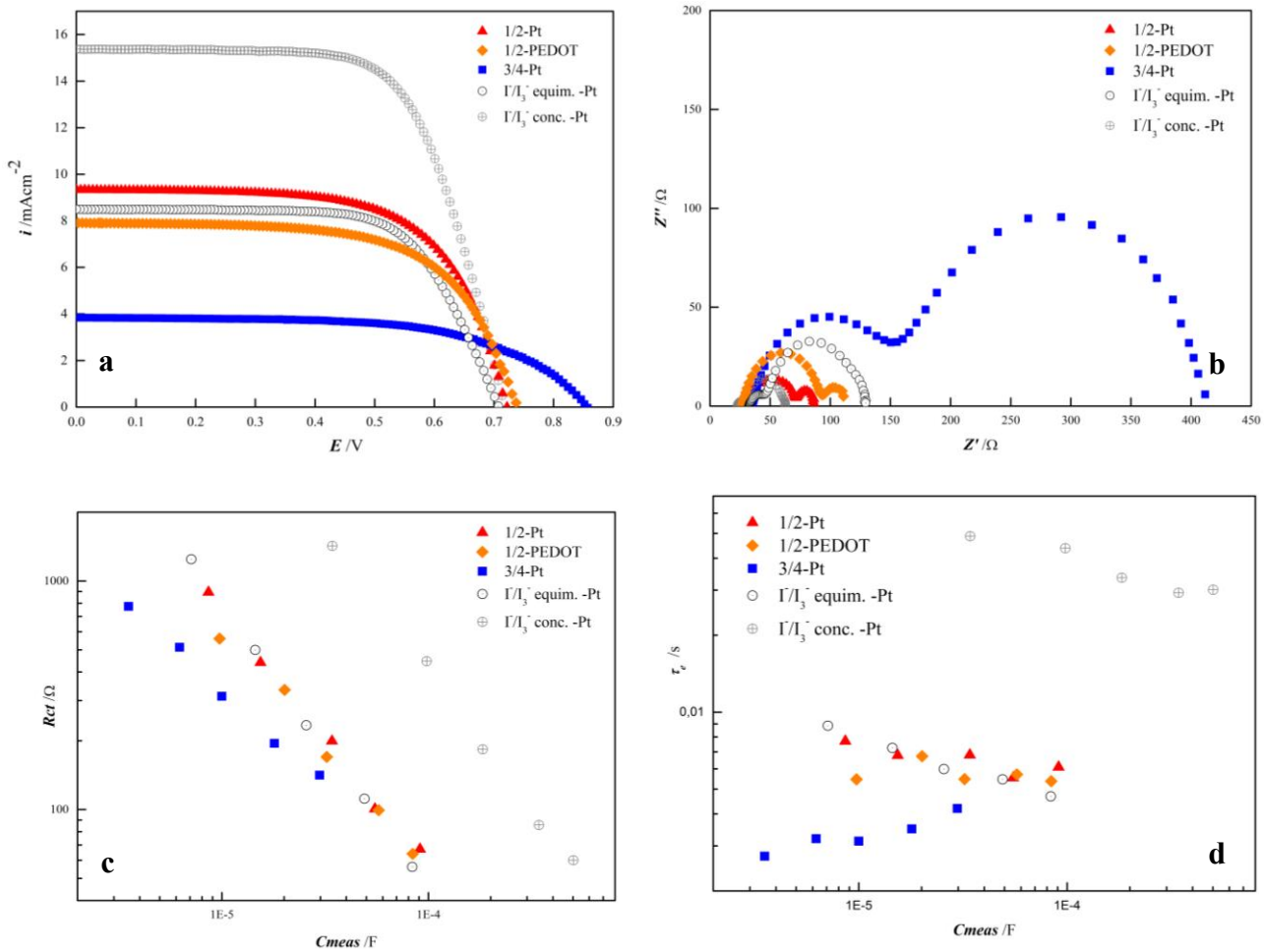

Fig. 6. a) *i*-*E* curves and b) Nyquist plots measured, at V_{oc} , under 1 sun illumination for **G3**-sensitized solar cells filled with the different electrolytes. c) charge transfer resistance, R_{ct}, and d) average lifetime of photogenerated electrons, τ_e, as a function of the measured capacitance, C_{meas}, of TiO_2 electrode.

However, to properly analyze the recombination process on the basis of comparable electron density values in the TiO_2, R_{ct} values have been plotted as a function of C_{meas} (Fig. 6c), where it emerges, on the contrary, the higher recombination resistance of **1**/**2**-EL, which lies at the basis of its higher performance. This finding is consistent with the quite inefficient dye regeneration by **3** resulting in a significant charge loss by direct back-recombination to the oxidized dye as well as the shorter electron lifetime ($\tau_e = R_{ct}C_{meas}$, Fig. 6d) of **3**/**4** with respect to **1**/**2** (around 4 and 6 ms at V_{oc}, respectively). The τ_e trends are even in good agreement with the observed trend of PCE (**$I^-/I_3^-$$_{conc}$** > **$I^-/I_3^-$$_{equim}$** ≈**1**/**2**-EL > **3**/**4**-EL).

Conclusions

In summary, the successful implementation in DSCs of an interesting class of redox mediators based on chemically engineered phenanthroline-based Cu complexes has been reported and rationalized on account of their electrochemistry and photoelectrochemistry. An increased energy barrier of the ET for the Cl-coordinated complex **4** with respect to its tetracoordinated analogue **2** has been clearly proven and associated to the higher reorganization energy associated to the Cu^{2+}/Cu^{+} redox process.

DSCs based on a properly formulated copper-phenanthroline electrolyte, **1**/**2** EL, in combination with a π-extended benzothiadiazole-based dye **G3**, shows a remarkable 4.4% PCE under 1 sun illumination, equating the performance of an equimolar **I^-/I_3^-** based EL. Even more promising is the doubling of cell performances respect to the benchmark **3**/**4** electrolyte, mainly attributable to the higher dye regeneration efficiency by **1** compared to **3**, and the faster Cu(I) regeneration at CE by **2** with respect to **4**. This last feature is driven by the lack of a fifth ancillary ligand (*i.e.*

Cl^-) in the exclusively tetracoordinated couple **1**/**2**. Unfortunately the cell performances of these Cu mediators are significantly limited by their lower solubility in ACN respect to the I^-/I_3^- couple; however further modifications to the ligands architecture and/or to the counteranion are expected to allow reducing this drawback, resulting in the development of a new class of iodine-free electron shuttles compatible with a wide spectrum of sensitizers, with the potentialities to outperform the current $[Cu(neocuproine)_2]^{2+/+}$ mediators.

ACKNOWLEDGMENTS

We thank Dr Stefano Chiaberge (Mass Spectrometry Lab, Renewable Energy and Environmental R&D, eni, Italy) for mass spectra characterization. This work was supported by MIUR (PRIN 2010-2011, 20104XET32, "DSSCX" and PON 02_00563_3316357, "MAAT"). The instrumentation purchased through the Regione Lombardia-Fondazione Cariplo joint SmartMatLab Project (grant numbers 12689/13, 7959/13; Azione 1 e 2) is gratefully acknowledged.

Supporting Information avaliable

http://pubs.acs.org: Synthesis and characterization of copper complexes; further experimental details; additional electrochemical characterizations of copper complexes; additional TA spectra and kinetic traces of G3 dye; additional characterization of devices (.pdf).

REFERENCES

(1) O'Regan, B.; Graetzel, M. *Nature* **1991**, *353*, 737-740.

(2) Hagfeldt A.; Boschloo G.,; Sun L.; Kloo L.; Pettersson H. *Chem. Rev.* **2010**, *110*, 6595-6663.

(3) Vougioukalakis G. C.; Philippopoulos A. I.; Stergiopoulos T.; Falaras P. *Coordin. Chem. Rev.* **2011**, *255*, 2602-2621.

(4) Chawla P.; Tripathi M. *Int. J. Energy Res.* **2015**, *39*, 1579-1596.

(5) Mahmood, A. *Sol. Energy* **2016**, *123*, 127-144.

(6) Chen, X.; Mao, S. S. *Chem. Rev.* **2007**, *107*, 2891-2959.

(7) Bignozzi, C. A.; Argazzi, R.; Boaretto, R.; Busatto, E.; Carli, S.; Ronconi, F.; Caramori, S. *Coord. Chem. Rev.* **2013**, *257*, 1472−1492.

(8) Wang, M. ; Graetzel, C.; Zakeeruddin, S. M.; Graetzel M. *Energy Environ. Sci.* **2012**, 5, 9394–9405.

(9) Hamann, T. W. *Dalton Trans.* **2012**, *41*, 3111−3115.

(10) Wu, J.; Lan, Z.; Lin, J.; Huang, M.; Huang, Y.; Fan, L.; Luo, L. *Chem. Rev.* **2015**, *115*, 2136-2173.

(11) Pashaei, B.; Shahroosvand, H.; Abbasi, P. *RSC Adv.* **2015**, *5*, 94814-94848.

(12) Li, T. C.; Spokoyny, A. M.; She, C. X.; Farha, O. K.; Mirkin, C. A.; Marks, T. J.; Hupp, J. T. *J. Am. Chem. Soc*. **2010**, *132*, 4580-4582.

(13) Daeneke, T.; Kwon, T. -H.; Holmes, A. B.; Duffy, N. W.; Bach, U.; Spiccia, L. *Nat. Chem*. **2011**, *3*, 211-215.

(14) Kakiage, K.; Aoyama, Y.; Yano, T.; Oya, K.; Fujisawab, J. -I.; Hanaya, M. *Chem. Commun.* **2015**, *51*, 15894-15897.

(15) Mathew, S.; Yella, A.; Gao, P.; Humphry-Baker, R.; Curchod, B.; Ashari-Astani, N.; Tavernelli, I.; Rothlisberger, U.; Nazeeruddin, M. K.; Graetzel, M. *Nat. Chem*. **2014**, *6*, 242-247.

(16) Yella, A.; Lee, H. -W.; Tsao, H. N.; Yi, C.; Chandiran, A. K.; Nazeeruddin, M. K.; Diau, E. W. -G.; Yeh, C. -Y.; Zakeeruddin, S. M.; Graetzel, M. *Science* **2011**, *334*, 629-634.

(17) Feldt, S. M.; Gibson, E. A.; Gabrielsson, E.; Sun, L.; Boschloo, G.; Hagfeldt, A. *J. Am. Chem. Soc*. **2010**, *132*, 16714-16724.

(18) Hattori, S.; Wada, Y.; Yanagida, S.; Fukuzumi, S. *J. Am. Chem. Soc.* **2005**, *127*, 9648−9654.

(19) Bai, Y.; Yu, Q.; Cai, N.; Wang, Y.; Zhang, M.; Wang, P. *Chem. Commun.* **2011**, *47*, 4376−4378.

(20) Colombo, A.; Dragonetti, C.; Magni, M.; Roberto, D.; Demartin, F.; Caramori, S.; Bignozzi, C. A. *ACS Appl. Mater. Interfaces* **2014**, *6*, 13945-13955 and references therein.

(21) Freitag, M.; Daniel, Q.; Pazoki, M.; Sveinbjörnsson, Z. J.; Sun, L.; Hagfeldt, A.; Boschloo, G. *Energy Environ. Sci*. **2015**, *8*, 2634-2637.

(22) Yu, Q.; Wang, Y.; Yi, Z.; Zu, N.; Zhang, J.; Zhang, M.; Wang, P. *ACS Nano* **2012**, 4, 6032–6038.

(23) Yum, J. -H.; Baranoff, E.; Kessler, F.; Moehl, T.; Ahmad, S.; Bessho, T.; Marchioro, A.; Ghadiri, E.; Moser, J. -E.; Yi, C.; Nazeeruddin, K.; Gratzel, M. *Nat. Commun.* **2012**, *3*, 1655/1-1655/8.

(24) Kashif, M. K.; Axelson, J. C.; Duffy, N. W.; Forsyth, C. M.; Chang, C. J.; Long, J. R.; Spiccia L.; Bach, U. *J. Am. Chem. Soc*. **2012**, *134*, 16646-16653.

(25) Kashif, M. K.; Nippe, M.; Duffy, N. W.; Forsyth, C. M.; Chang, C. J.; Long, J. R.; Spiccia, L.; Bach, U. *Angew. Chem. Int. Ed*. **2013**, *52*, 5527–55.

(26) Giribabu, L.; Bolligarla, R.; Panigrahi, M. *Chem. Rec.* **2015**, *15*, 760-788.

(27) Ye, M.; Wen, X; Wang, M.; Iocozzia, J.; Zhang, N.; Lin, C.; Lin, Z. *Mat. Today* **2015**, *18*, 155-162.

(28) Clifford, J. N.; Martinez-Ferrero, E.; Palomares, E. *J. Mater. Chem*. **2012**, *22*, 12415-12422.

(29) Sykes, A.G. *Adv. Inorg. Chem.* **1991**, *36*, 377-408.

(30) Magni, M.; Colombo, A.; Dragonetti, C.; Mussini, P. *Electrochim. Acta* **2014**, *141*, 324-330.

(31) Grisorio, R.; De Marco, L.; Baldisserri, C.; Martina, F.; Serantoni, M.; Gigli, G.; Suranna, G. P. *Sustainable Chem. Eng.* **2015**, *3*, 770-777.

(32) Gritzner, G.; Kuta, J. *Pure Appl. Chem*. **1984**, *56*, 461-466.

(33) Sharmoukh, W.; Attanzio, A.; Busatto, E.; Thibaud, E.; Carli, S.; Monari, A.; Assfeld, X.; Beley, M.; Caramori, S.; Gros, P. C. *RSC Adv*., **2015**, *5*, 4041-4050.

(34) Ichinaga, A. K.; Kirchhoff, J. R.; McMillin, D. R.; Dietrich-Buchecker, C. O.; Marnot, P. A.; Sauvage, J.4 -P. *Inorg. Chem.* **1987**, *26*, 4290-4292.

(35) Phifer C. C.; McMillin, D. R. *Inorg. Chem*. **1986**, *25*, 1329-1333.

(36) Armaroli, N. *Chem. Soc. Rev*. **2001**, *30*, 113-124.

(37) Schlichthorl, G.; Huang, S.; Sprague, J.; Frank, A. *J. Phys. Chem. B* **1997**, *101*, 8141-8155.

(38) Goldsmith, C. R.; Jonas, R. T.; Cole, A. P.; Stack T. D. P. *Inorg. Chem.* **2002**, *41*, 4642-4652.

(39) Randles, J. E. B. *Discuss. Faraday Soc*. **1947**, *1*, 11-19.

(40) Hao, F.; Dong, P.; Luo, Q.; Li, J.; Lou, J.; Li, H. *Energy Environ. Sci.* **2013**, *6,* 2003-2019.

(41) Yun, S.; Hagfeldt, A.; Ma, T. *Adv. Mater.* **2014,** *26*, 6210-6237.

(42) Xu, M.; Zhou, D.; Cai, N.; Liu, J.; Li, R.; Wang P. *Energy Environ. Sci.* **2011**, *4*, 4735-4742.

(43) Mba, M.; D'Acunzo, M.; Salice, P.; Carofiglio, T.; Maggini, M.; Caramori, S.; Campana, A.; Aliprandi, A.; Argazzi, R.; Carli, S.; Bignozzi, C. A. *J. Phys.Chem. C* **2013**, *117*, 19885-19896.

(44) Fabregat-Santiago, F.; Bisquert, J.; Garcia-Belmonte, G.; Boschloo, G.; Hagfeldt, A. *Sol. Energ. Mater. Solar C*. **2005**, *87*, 117-131.

(45) Fabregat-Santiago, F.; Bisquert, J.; Palomares, E.; Otero, L.; Kuang, D.; Zakeeruddin, S. M.; Grätzel, M.. *J. Phys. Chem. C* **2007**, *111*, 6550-6560.

For Table of Contents Only

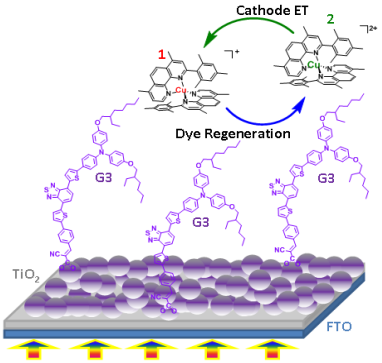

A tetracoordinated redox couple, made of [Cu(2-mesityl-4,7-dimethyl-1,10-phenanthroline)$_2$][PF_6] and its Cu(II) form, has been synthesized and its electrochemical and photoelectrochemical features investigated. The new redox mediators doubled the cell efficiency obtained with the benchmark redox couple, [Cu(2,9-dimethyl-1,10-phenanthroline)$_2$][PF_6] and its chloride-coordinated cupric form, giving results comparable to an equimolar I^-/I_3^--based electrolyte.